International Journal of Heat and Mass Transfer 52 (2009) 4279–4295

Contents lists available at ScienceDirect

International Journal of Heat and Mass Transfer

journal homepage: www.elsevier.com/locate/ijhmt

Electroosmotic flow driven by oscillating zeta potentials: Comparison of the Poisson–Boltzmann model, the Debye–Hückel model and the Nernst–Planck model

H.M. Park *, Y.J. Choi

Department of Chemical and Biomolecular Engineering, Sogang University, Seoul, South Korea

ARTICLE INFO

Article history:
Received 17 November 2008
Received in revised form 2 April 2009
Accepted 2 April 2009
Available online 6 June 2009

Keywords:
Electroosmotic flow
Poisson–Boltzmann model
Nernst–Planck model
Debye–Hückel model

ABSTRACT

We consider electroosmotic flows (EOF) generated by temporally varying zeta potential which is usually adopted for pumping or mixing of fluids. In this case the dynamics of ions in the electric double layer (EDL) influences the induced electric field and consequently the EOF significantly. Therefore, the appropriate model should be the Nernst–Planck (NP) model for all zeta potentials or the Debye–Hückel (DH) model for low zeta potentials rather than the Poisson–Boltzmann (PB) model which is based on the equilibrium distribution of ions in the EDL. In the present investigation, we compare the predictions from the DH model and the PB model with the exact ones from the NP model for a range of frequency of zeta potential oscillation. It is found that one may adopt the PB model when the frequency is low and the DH model when the zeta potential is low. However, for either high frequency of zeta potential oscillation or large value of zeta potential, one must adopt the NP model to get accurate predictions of EOF.

1. Introduction

Recently there have been a renewed interest in electroosmotic flow in capillaries due to its relevance to many microfluidic systems based on the lab-on-a-chip concept. In these microfluidic systems the target chemical species are delivered by activating electroosmotic flow. Electroosmotic flow is induced when an electric field is imposed through the electric double layer, where the separation of positive and negative ions occurs because of the zeta potential at the microchannel wall [1]. The electric force acting on these ions is the driving force of the electroosmotic flow. Usually, one of the following three models is adopted in the analysis of electroosmotic flows; the Nernst–Planck (NP) model, the Debye–Hückel (DH) model and the Poisson–Boltzmann (PB) model. In the Nernst–Planck model the conservation equations for the cations and anions are solved coupled with the Navier–Stokes equation to find the electric potential in the electric double layer induced by ionic unbalance near the wall. Though the most rigorous model, it is difficult to solve the NP model numerically due to the strong nonlinear couplings between velocity, cation concentration, anion concentration and the electric potential induced by the ionic unbalance. A commonly accepted approximation to the Nernst–Planck model is the Debye–Hückel model. The DH model can be derived from the NP model when the zeta potential is small. Under many circumstances the ionic distribution in the electric double layer is not disturbed at a fixed zeta potential, and it follows the equilibrium Boltzmann distribution. In these cases the induced electric field is governed by the Poisson–Boltzmann equation and is decoupled from the velocity field, resulting in the Poisson–Boltzmann model which is the most widely employed model in the analysis of electroosmotic flows due to its simplicity. For a fixed zeta potential, the predictions of the PB model agree with those of the NP model at small values of the Debye length, which occur at large zeta potential and high ionic concentrations [2].

However, there have been attempts to vary wall zeta potential directly by imposing external electric field at the microchannel wall to control electroosmotic flows. When an electric field is applied perpendicular to the channel, a radial electric potential gradient is created across the insulating channel wall that allows for direct control of the zeta potential and the resulting electroosmotic flow. The use of ultrathin insulating walls allows significantly small voltages to create extraordinary fields required to have effective field-effect flow control [3–6]. It is also found that application of a AC voltage across the channel wall generates electroosmotic flows, resulting in pumping or mixing of fluids [7–10]. For the analysis of electroosmotic flows generated by the temporally varying zeta potential, as in the above applications, most investigators have adopted the Debye–Hückel model which permits analytic solutions in certain flow configurations [7,8]. However, the DH model is valid only for small values of zeta potential. In the present investigation, we compare the induced potential and velocity fields obtained from the Nernst–Planck model, the Debye–Hückel model and the Poisson–Boltzmann model systematically when the zeta potential varies sinusoidally at various frequencies, and suggest the range of validity of the DH and PB models.

* Corresponding author. Tel.: +82 2 705 8482.
E-mail address: hmpark@sogang.ac.kr (H.M. Park).

0017-9310/$ - see front matter © 2009 Elsevier Ltd. All rights reserved.
doi:10.1016/j.ijheatmasstransfer.2009.04.022

Nomenclature

D	diffusivity of ions
e	elementary charge
J^+	cationic current
J^-	anionic current
k_B	Boltzmann constant
L	characteristic length of the system
N	difference between anionic and cationic concentration $(n^- - n^+)$
n_0	bulk ionic concentration
n^+	cationic concentration
n^-	anionic concentration
P	pressure
Re	Reynolds number
Sc	Schmidt number
T	temperature
t	time
U	characteristic velocity of the system
$\mathbf{v}$	velocity vector
v^z	axial velocity
y	normal direction to the wall
z	valence of ions

Greek symbols

α	parameter defined in Eq. (6)
β	parameter defined in Eq. (6)
δ	parameter defined in Eq. (6)
ϵ_0	permittivity of vacuum
ϵ	dielectric constant
ζ_0	reference zeta potential
ζ	zeta potential
κ	Debye length
μ	viscosity
ρ	fluid density
ϕ	external electric potential
ψ	induced electric potential
ω	frequency of zeta potential oscillation

2. Models of electroosmotic flows

For simple electrolytes that dissociate into two equally charged ions of valence z and $-z$, the dimensionless governing equations for electroosmotic flows may be written under the assumption of the Gouy–Chapman model as [2,11].

$$\frac{\partial n^{+*}}{\partial t^*} + \mathbf{v}^* \cdot \nabla n^{+*} = \frac{1}{ScRe}\nabla^{*2} n^{+*} + \frac{\alpha}{ScRe}\nabla^* \cdot (n^{+*}\nabla^*\psi^*) + \frac{\alpha}{ScRe}\nabla^* \cdot (n^{+*}\nabla^*\phi^*) \tag{1}$$

$$\frac{\partial n^{-*}}{\partial t^*} + \mathbf{v}^* \cdot \nabla n^{-*} = \frac{1}{ScRe}\nabla^{*2} n^{-*} - \frac{\alpha}{ScRe}\nabla^* \cdot (n^{-*}\nabla^*\psi^*) - \frac{\alpha}{ScRe}\nabla^* \cdot (n^{-*}\nabla^*\phi^*) \tag{2}$$

$$\nabla^{*2}\psi^* = \frac{\beta}{2}(n^{-*} - n^{+*}) \tag{3}$$

$$\frac{\partial \mathbf{v}^*}{\partial t^*} + \mathbf{v}^* \cdot \nabla \mathbf{v}^* = -\nabla^* P^* + \frac{1}{Re}\nabla^{*2}\mathbf{v}^* + \delta(n^{-*} - n^{+*})\nabla^*\phi^* \tag{4}$$

$$\nabla^* \cdot \mathbf{v}^* = 0 \tag{5}$$

In the above equations the dimensionless variables have been defined as follows:

$$\mathbf{x}^* = \frac{\mathbf{x}}{L}, \quad \psi^* = \frac{\psi}{\zeta_0}, \quad \mathbf{v}^* = \frac{\mathbf{v}}{U}, \quad P^* = \frac{P}{\rho_f U^2}, \quad t^* = \frac{tU}{L},$$

$$\phi^* = \frac{\phi}{\zeta_0}, \quad n^{+*} = \frac{n^+}{n_0}, \quad n^{-*} = \frac{n^-}{n_0}, \quad w = \frac{1}{\kappa} = \sqrt{\frac{8\pi n_0 e^2 z^2}{\varepsilon_0 \varepsilon k_b T}},$$

$$\alpha = \frac{ez\zeta_0}{k_B T}, \quad \beta = \frac{(wL)^2}{\alpha} = \frac{L^2 2n_0 ez}{\varepsilon_0 \varepsilon \zeta_0}, \quad \delta = \frac{zen_0\zeta_0}{\rho_f U^2},$$

$$Re = \frac{\rho_f LU}{\mu}, \quad Sc = \frac{\mu}{\rho_f D} \tag{6}$$

where, n^+ is the number concentration of the cation, n^- is that of the anion, D is the diffusivity of ions, z is the valence, e is the elementary charge, k_B is the Boltzmann constant, T is the absolute temperature, ψ is the local electric potential induced by ions, ϕ is the externally imposed electric potential, $\mathbf{v}$ is the velocity, ρ_f is the fluid density, P is the pressure, μ is the viscosity, ε_0 is the permittivity of the vacuum and ε is the dielectric constant, L is the width of the microchannel, n_0 is the bulk ionic concentration and ζ_0 is the surface electric potential, which is taken to be the same as the zeta potential, at a reference position and κ is the Debye length characterizing the depth of the electric double layer. The electroosmotic flow model composed of Eqs. (1)–(5) is called the Nernst–Planck (NP) model. Eqs. (1) and (2) represent the conservation equations for the cations and anions, both of which induce electric field ψ^* in the electric double layer. Eq. (3) shows that the ionic unbalance in the electric double layer gives rise to the induced potential ψ^*. The ionic unbalance also acts as a body force in the momentum Eq. (4) when there is external potential gradient $\nabla^*\phi^*$. The Nernst–Planck model takes care of the dynamic effects of ions and is the most rigorous model to be considered in the present investigation. From now on, we delete the asterisk indicating dimensionless variables for the sake of brevity.

Next, we show conditions under which the Debye–Hückel model is derived from the NP model. When the values of α is small, which corresponds to a weak zeta potential, we may approximate the dimensionless ionic fluxes as follows:

$$J^\pm \equiv \mathbf{v}n^\pm - \frac{1}{ScRe}\nabla n^\pm - \frac{z^\pm\alpha}{ScRe}n^\pm(\nabla\psi + \nabla\phi) \approx \mathbf{v}n^\pm - \frac{1}{ScRe}\nabla n^\pm - \frac{z^\pm\alpha}{ScRe}(\nabla\psi + \nabla\phi) \tag{7}$$

since the contribution of the last term in the right hand side of the above equation is not significant compared with other terms. Then the last two terms of Eqs. (1) and (2) are approximated as

$$\frac{\alpha}{ScRe}\nabla \cdot (n^\pm\nabla\psi) = \frac{\alpha}{ScRe}\nabla^2\psi; \quad \frac{\alpha}{ScRe}\nabla \cdot (n^\pm\nabla\phi) = \frac{\alpha}{ScRe}\nabla^2\phi \tag{8}$$

Defining a new variable N such that

$$N \equiv n^- - n^+ \tag{9}$$

and exploiting the fact that the external potential ϕ satisfies $\nabla^2\phi = 0$, the set of equations defining the NP model, Eqs. (1)–(4), reduces to the following set of equations called the Debye–Hückel (DH) model:

$$\frac{\partial N}{\partial t} + \mathbf{v} \cdot \nabla N = \frac{1}{ScRe}\nabla^2 N - \frac{\alpha\beta}{ScRe}N \tag{10}$$

$$\frac{\partial \mathbf{v}}{\partial t} + \mathbf{v} \cdot \nabla \mathbf{v} = -\nabla P + \frac{1}{Re}\nabla^2\mathbf{v} + N\delta\nabla\phi \tag{11}$$

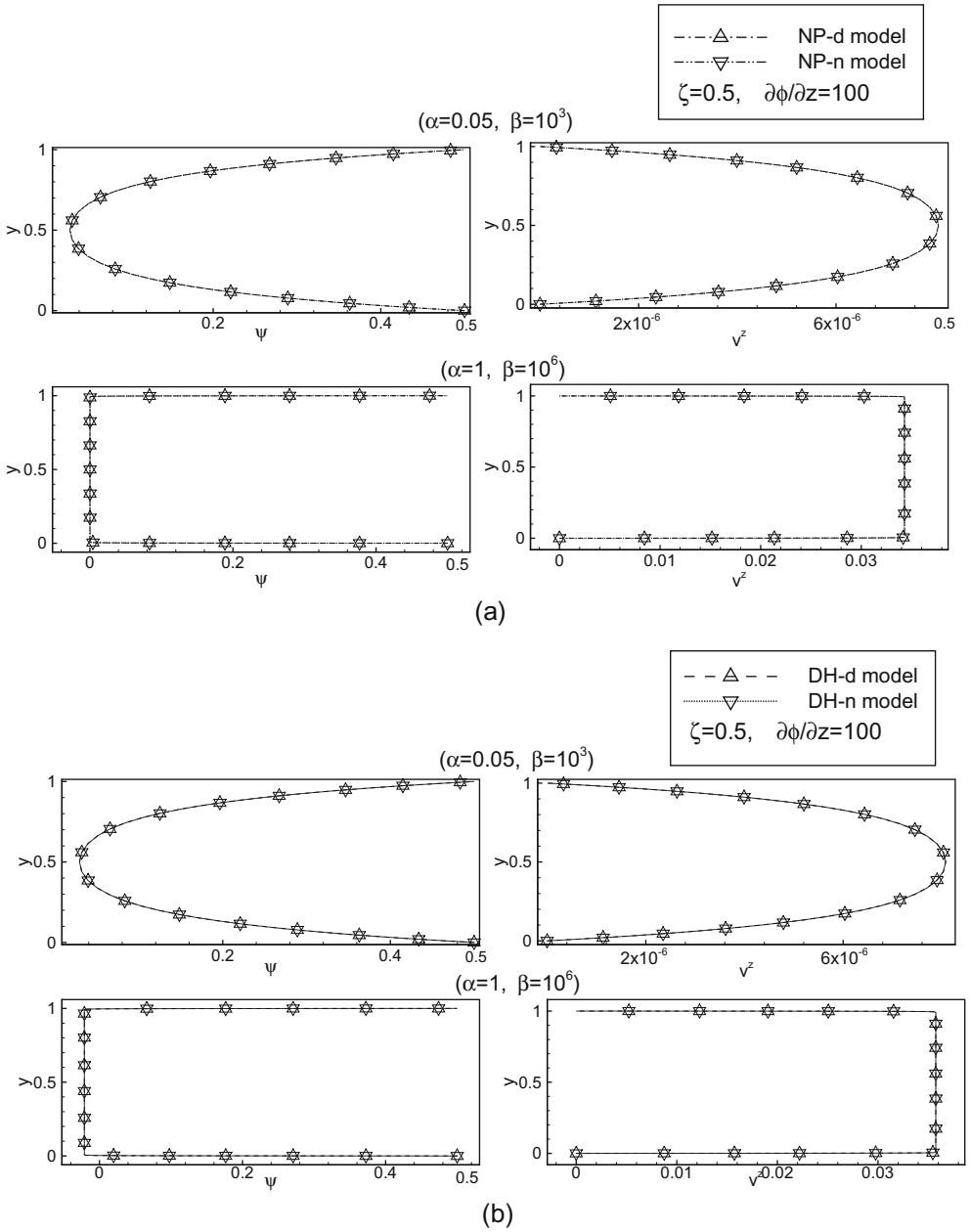

Fig. 1. Effect of boundary conditions (a) the comparison of NP-d and NP-n models and (b) the comparison of DH-d and DH-n models.

In the DH model, the electroosmotic body force in the momentum equation is given by N and the induced potential ψ is not need. If we need the ψ field, it can be found by solving the following equation a posteriori.

$$\nabla^2\psi = \frac{\beta}{2}N \tag{12}$$

The DH model permits analytic solution because it is linear in N, even though it takes care of the ionic transport. Thus many investigators have adopted the DH model to study the effect of the deviation of ionic distributions from the equilibrium ones, although the DH model is valid only at small zeta potential values.

Another approximation of the NP model is the Poisson–Boltzmann model which is derived under the condition that ionic distributions in the electric double layer is in equilibrium, which is valid when the convective transport of ions is negligible and ionic distribution is at the steady state within a very thin electric double layer. Under these assumptions, Eqs. (1) and (2) are easily integrated to the following analytic expressions.

$$n^+ = \exp(-\alpha\psi), \quad n^- = \exp(\alpha\psi) \tag{13}$$

In the above derivation, we implicitly adopt the boundary conditions such that $\nabla\psi = 0$, $\psi = 0$, $\nabla n^{\pm} = 0$, $n^{\pm} = 1$ at the far field from the channel walls, which are valid if the electric double layer does not overlap at the center of the microchannel. Substituting Eq. (13) into Eq. (3), we find the Poisson–Boltzmann equation for the induced electric potential ψ:

$$\nabla^2\psi = \beta\sinh(\alpha\psi) \tag{14}$$

Using Eqs. (13) and (4) becomes

$$\frac{\partial \mathbf{v}}{\partial t} + \mathbf{v}\cdot\nabla\mathbf{v} = -\nabla P + \frac{1}{Re}\nabla^2\mathbf{v} + 2\delta\sinh(\alpha\psi)\nabla\phi \tag{15}$$

Eqs. (13)–(15) constitute the Poisson–Boltzmann (PB) model. The PB model is valid even for large values of zeta potential and high

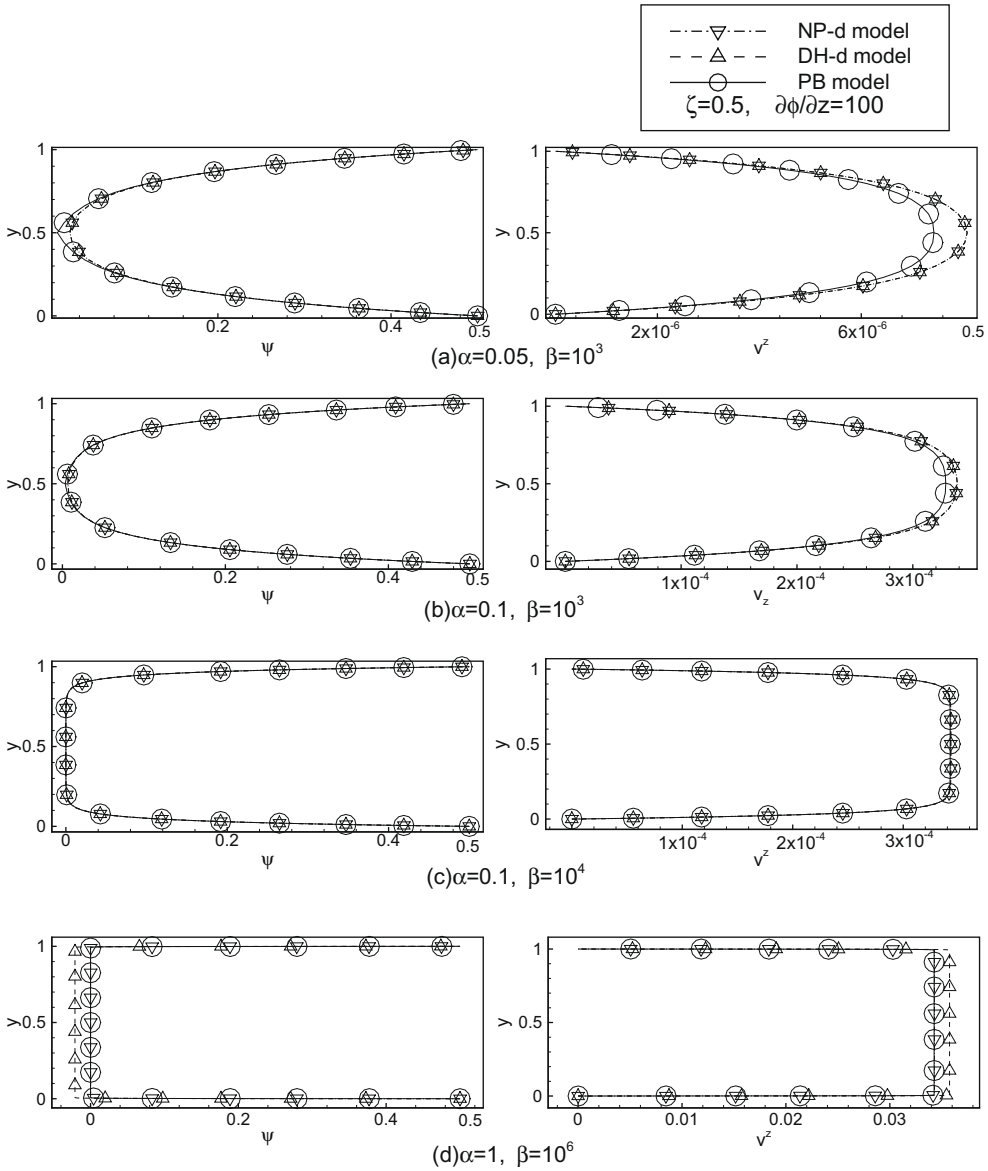

Fig. 2. Comparison of the steady state velocity and induced electric potential ψ predicted by various models when $\zeta = 0.5$ and $\partial\phi/\partial z = 100$. (a) $\alpha = 0.05, \beta = 10^3$, (b) $\alpha = 0.1, \beta = 10^3$, (c) $\alpha = 0.1, \beta = 10^4$ and (d) $\alpha = 1.0, \beta = 10^6$.

bulk ionic concentration, which corresponds to a thin electric double layer. However, it does not take care of the convective transport and the transient behavior of ionic concentrations.

3. Comparison of the Nernst–Planck model, the Debye–Hückel model and the Poisson–Boltzmann model

We consider a long straight slit microchannel without pressure gradient under a constant external electric field where the spatially homogeneous zeta potential varies temporally, which induces electroosmotic flows. Typical parameter values for the electroosmotic flows in various microfluidic devices are:

$$z = 1, \quad \zeta_0 = 0.1V, \quad T = 298\,K, \quad L = 10^{-4}m,$$
$$\epsilon_r = 78.5, \quad U = 8 \times 10^{-4}ms^{-1}, \quad n_0 = 10^{-4}molL^{-1} \tag{16}$$

For the above parameter values, it is found that

$$\alpha = 3.89, \quad \beta = 2.777 \times 10^6, \quad \delta = 2.85 \times 10^{-3}\alpha^2\beta, \quad Re = 0.1, \tag{17}$$

and the Debye length κ given by $L/\sqrt{\alpha\beta}$ is less than one thousandth of the channel width. The Schmidt number Sc for cations and anions is taken to be the same value 400, which corresponds to the case of K^+ and Cl^- approximately. Since the bulk ionic concentration n_0 affects β, we find that κ increases a threefold if n_0 decreases ten times. Around the central region of the microchannel where the end effects are negligible, the following conditions are valid:

$$v^x = v^y = 0, \quad \frac{\partial}{\partial z} = 0 \tag{18}$$

where z is the axial direction and x and y are the cross-sectional coordinates of the microchannel. Under the conditions of Eq. (18), the continuity Eq. (5) is satisfied automatically and the convective transport terms in the above equations, $\mathbf{v}\cdot\nabla n^{\pm}$, $\mathbf{v}\cdot\nabla N$ and $\mathbf{v}\cdot\nabla\mathbf{v}$, vanish. Then the velocity, the ionic concentrations and the internal electric potential vary only in the normal direction to the microchannel walls. Let y denote the normal direction to the microchannel wall. The governing equations and relevant boundary conditions for the NP model, the DH model and the PB model may be written as follows:

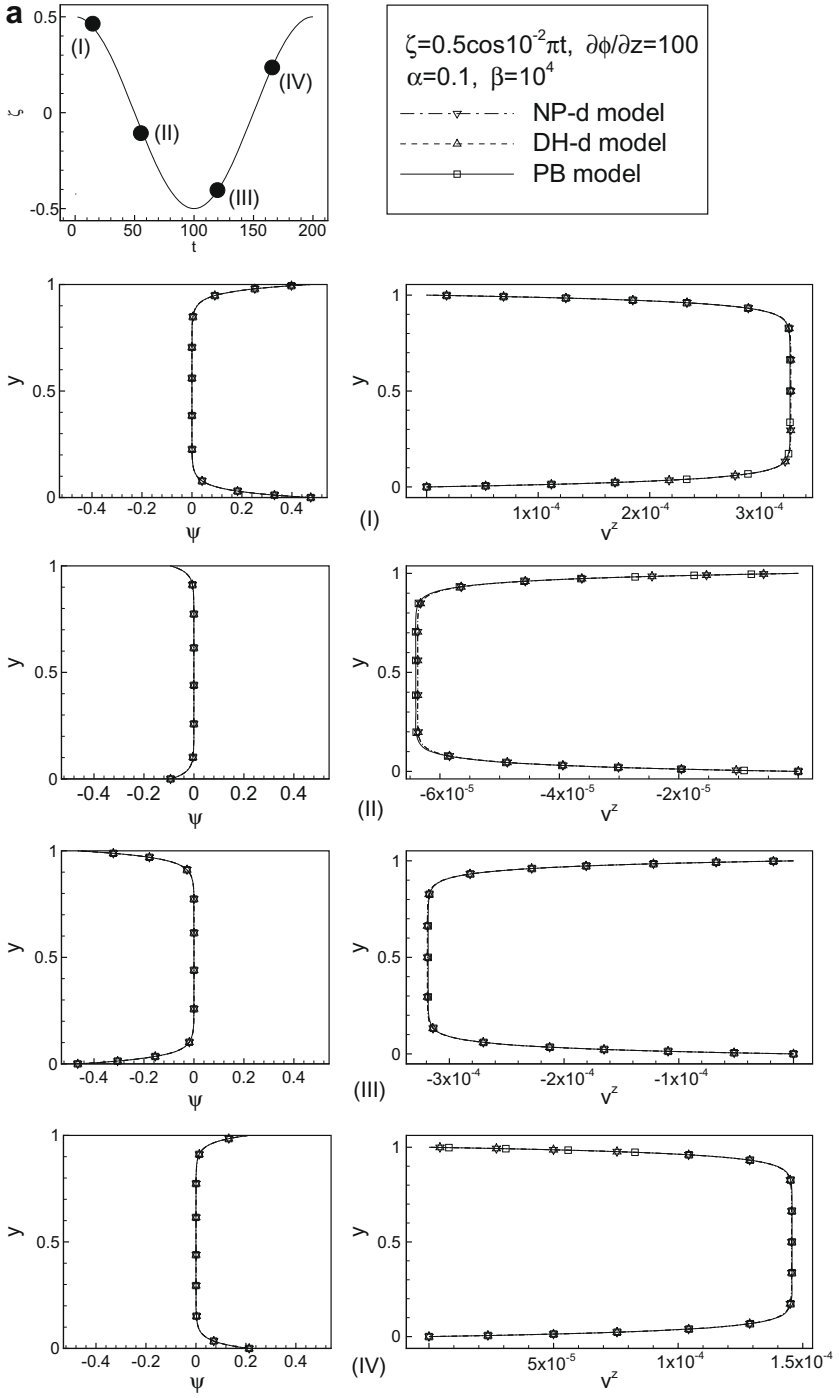

Fig. 3. (a) Comparison of the induced electric potential ψ and v^z predicted by various models when $\zeta = 0.5\cos 10^{-2}\pi t$ and $(\alpha, \beta) = (0.1, 10^4)$. (b) Comparison of the induced electric potential ψ and v^z predicted by various models when $\zeta = 0.5\cos 10\pi t$ and $(\alpha, \beta) = (0.1, 10^4)$. (c) Comparison of the induced electric potential ψ and v^z predicted by various models when $\zeta = 0.5\cos 10^4\pi t$ and $(\alpha, \beta) = (0.1, 10^4)$.

NP model

$$\frac{\partial n^+}{\partial t} = \frac{1}{ScRe}\frac{\partial^2 n^+}{\partial y^2} + \frac{\alpha}{ScRe}\frac{\partial}{\partial y}\left(n^+\frac{\partial \psi}{\partial y}\right) \tag{19}$$

$$\frac{\partial n^-}{\partial t} = \frac{1}{ScRe}\frac{\partial^2 n^-}{\partial y^2} - \frac{\alpha}{ScRe}\frac{\partial}{\partial y}\left(n^-\frac{\partial \psi}{\partial y}\right) \tag{20}$$

$$\frac{\partial^2 \psi}{\partial y^2} = \frac{\beta}{2}(n^- - n^+) \tag{21}$$

$$\frac{\partial v^z}{\partial t} = \frac{1}{Re}\frac{\partial^2 v^z}{\partial y^2} + \delta(n^- - n^+)\frac{\partial \phi}{\partial z} \tag{22}$$

with the following boundary conditions.

- $y = 0;\quad n^+ = e^{-\alpha\zeta},\quad n^- = e^{\alpha\zeta},\quad \psi = \zeta,\quad v^z = 0$ (23)
- $y = 1.0;\quad n^+ = e^{-\alpha\zeta},\quad n^- = e^{\alpha\zeta},\quad \psi = \zeta, v^z = 0$ (24)

Since the boundary conditions, Eqs. (23) and (24), are symmetric with respect to $y = 1/2$ and the solution of Eqs. (19)–(22) are $n^+ = 1,\ n^- = 1,\ \psi = 0,\ \frac{\partial v^z}{\partial y} = 0$ in the bulk flow domain, the boundary conditions given by Eq. (24) are imposed by setting $n^+ = 1,\ n^- = 1,\ \psi = 0,\ \frac{\partial v^z}{\partial y} = 0$ at $y = 5$–6κ, where κ is the Debye length. The boundary conditions Eq. (23) are based on the assumption that the ionic concentrations are in equilibrium at the wall. However,

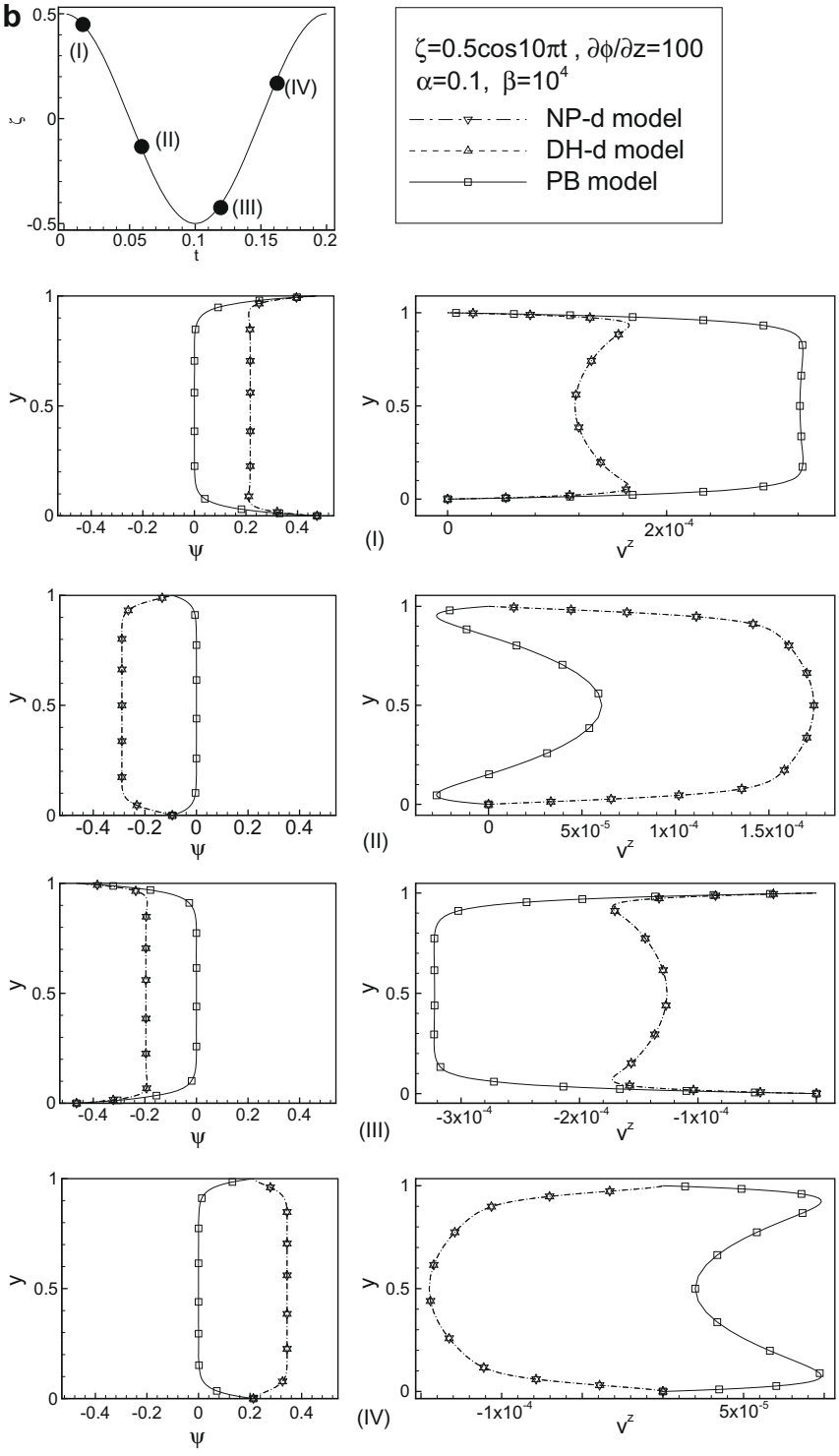

Fig. 3 (*continued*)

a more rigorous boundary conditions may be the imposition of no ionic fluxes at the wall expressed as follows.

$$\bullet\, y=0;\ \frac{\partial n^+}{\partial y}+\alpha n^+\frac{\partial \psi}{\partial y}=0,\ \frac{\partial n^-}{\partial y}-\alpha n^-\frac{\partial \psi}{\partial y}=0,\qquad \psi=\zeta,\ v^z=0 \tag{25}$$

In the sequel, we call Eq. (23) the Dirichlet boundary conditions and Eq. (25) the Neumann boundary conditions. The set of Eqs. (19)–(21), which are strongly coupled, and relevant boundary conditions is discretized by a finite difference method, and the resulting nonlinear algebraic equations are solved at each time step using the Newton–Raphson method when ζ varies temporally. Once n^- and n^+ are obtained at a given time step, the axial velocity v^z, governed by the linear Eq. (22), is easily found using a finite difference method.

DH model

$$\frac{\partial N}{\partial t}=\frac{1}{ScRe}\frac{\partial^2 N}{\partial y^2}-\frac{\alpha\beta}{ScRe}N \tag{26}$$

$$\frac{\partial^2 \psi}{\partial y^2}=\frac{\beta}{2}N \tag{27}$$

$$\frac{\partial v^z}{\partial t}=\frac{1}{Re}\frac{\partial^2 v^z}{\partial y^2}+\delta N\frac{\partial \phi}{\partial z} \tag{28}$$

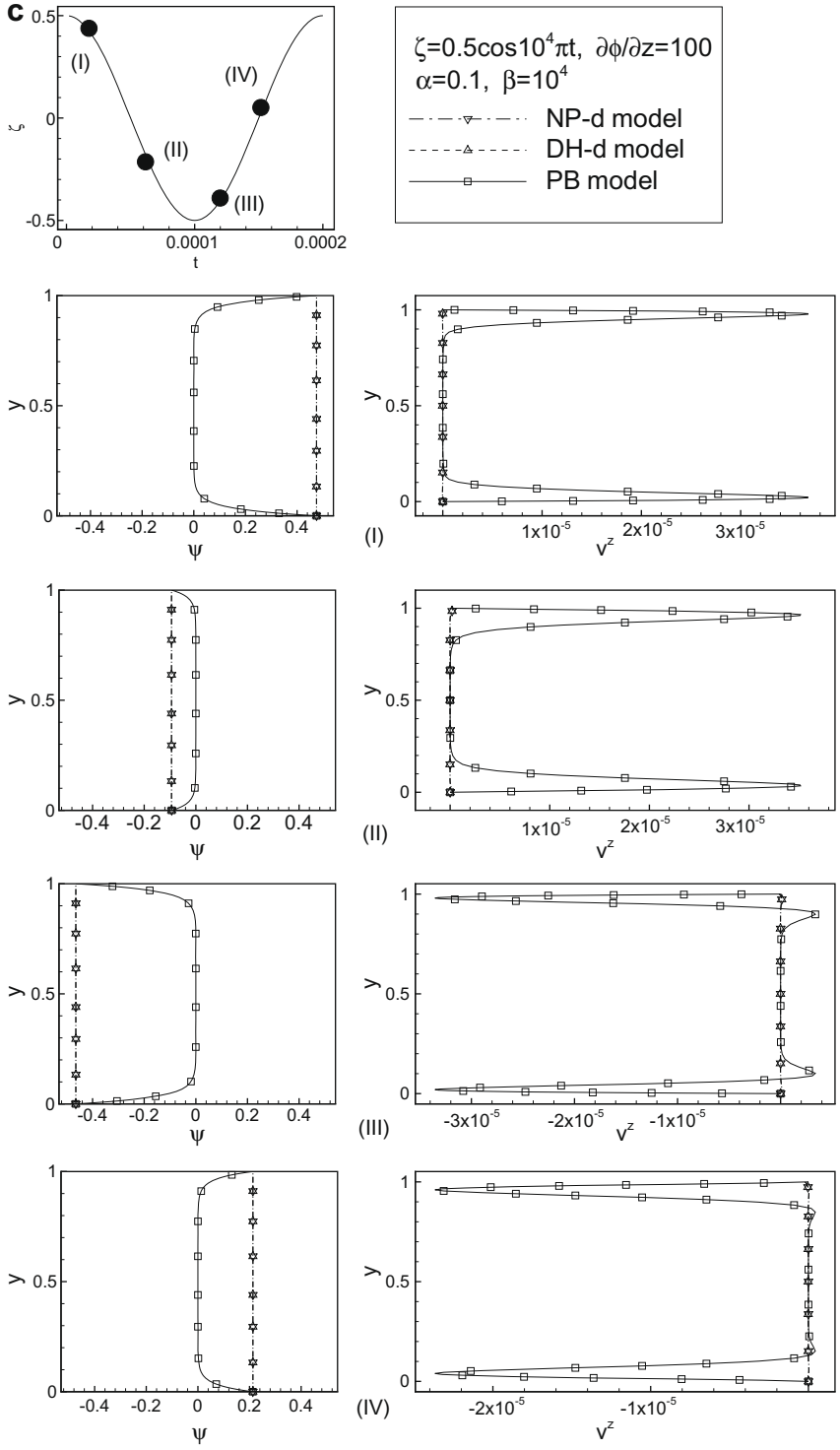

Fig. 3 (*continued*)

with the following boundary conditions.

$$\bullet\, y = 0; \quad N = e^{\alpha\zeta} - e^{-\alpha\zeta}, \quad \psi = \zeta, \quad v^z = 0 \tag{29}$$

$$\bullet\, y = 1.0; \quad N = e^{\alpha\zeta} - e^{-\alpha\zeta}, \quad \psi = \zeta, \quad v^z = 0 \tag{30}$$

Eq. (29) represents the Dirichlet boundary conditions where the equilibrium ionic distributions are assumed. The Neumann boundary conditions corresponding to the no ionic fluxes at the wall may be written as follows

$$\bullet\, y = 0; \quad \frac{\partial N}{\partial y} + 2\alpha\frac{\partial \psi}{\partial y} = 0, \quad \psi = \zeta, \quad v^z = 0 \tag{31}$$

Since the ionic flux is approximated by Eq. (7) in the Debye–Hückel model, Eq. (31) results from Eq. (25). Eq. (29) is the Dirichlet boundary conditions for the DH model while Eq. (31) is the Neumann boundary conditions for the same model. Since Eq. (26) is a linear equation for N, it can be solved easily using a finite difference method. Once N is found at a given time step, Eq. (28) is solved using a finite difference method to find the axial velocity v^z. If the potential

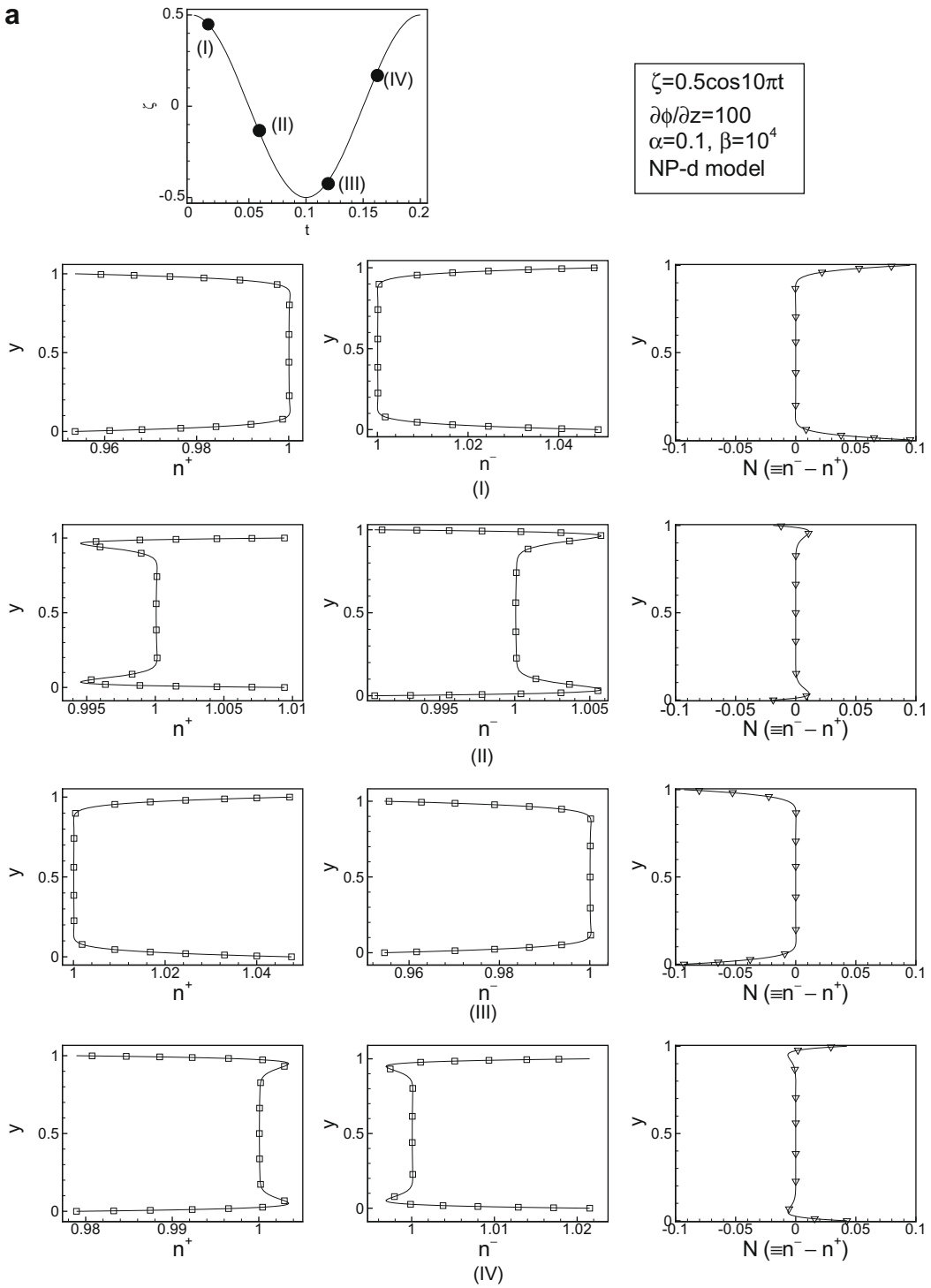

Fig. 4. (a) Variation of n^-, n^+ and $N(\equiv n^- - n^+)$ predicted by the NP-d model when $\zeta = 0.5\cos 10\pi t$ and $(\alpha, \beta) = (0.1, 10^4)$. (b) Variation of n^-, n^+ and $N(\equiv n^- - n^+)$ predicted by the NP-d model when $\zeta = 0.5\cos 10^4\pi t$ and $(\alpha, \beta) = (0.1, 10^4)$.

ψ is needed, it is found by solving Eq. (27) using N at the same time step. We may employ either the Dirichlet or Neumann boundary conditions at the wall.

PB model

$$\frac{\partial^2\psi}{\partial y^2} = \beta\sinh(\alpha\psi) \tag{32}$$

$$\frac{\partial v^z}{\partial t} = \frac{1}{Re}\frac{\partial^2 v^z}{\partial y^2} + 2\delta\sinh(\alpha\psi)\frac{\partial\phi}{\partial z} \tag{33}$$

$$\bullet\, y = 0, 1; \psi = \zeta, v^z = 0 \tag{34}$$

The boundary condition at y=1 may be replaced with

$$\bullet y = 5\text{–}6\kappa; \quad \psi = 0, \quad \frac{\partial v^z}{\partial y} = 0 \tag{35}$$

when the Debye length is very small.

Contrary to the NP model and the DH model, the PB model cannot take care of the dynamics of the electric potential ψ. Whenever the zeta potential varies, its effect on ψ appears instantaneously in the PB model. One can find analytic solution of Eq. (32) with the

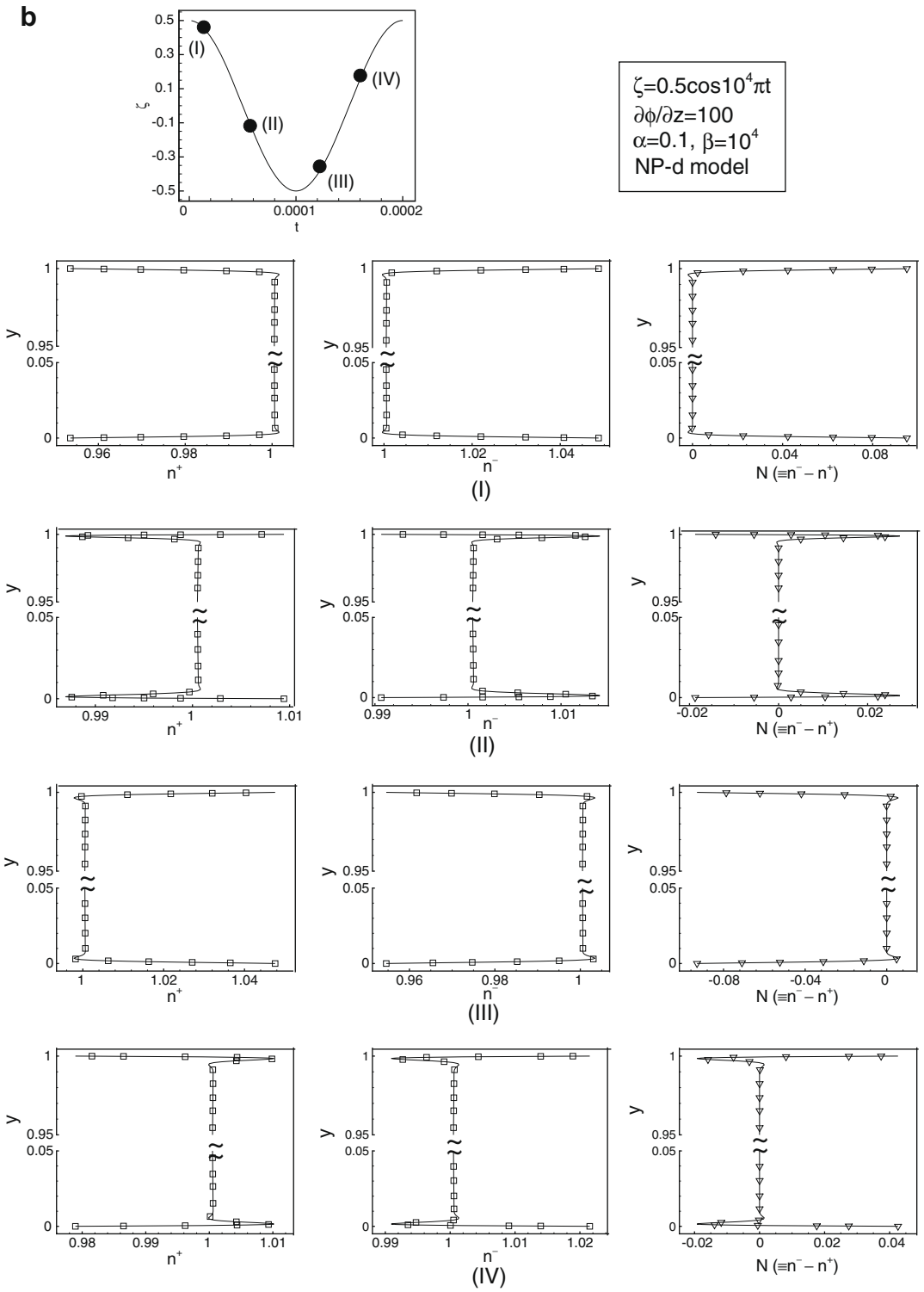

Fig. 4 (*continued*)

relevant boundary conditions given by Eqs. (34) and (35) as follows.

$$\psi = \frac{2}{\alpha}\ln\left[\frac{1+e^{-\sqrt{\alpha\beta}y}\tanh\left(\frac{\alpha}{4}\zeta\right)}{1-e^{-\sqrt{\alpha\beta}y}\tanh\left(\frac{\alpha}{4}\zeta\right)}\right] \tag{36}$$

First, we compare the NP-d model with the NP-n model and the DH-d model with the DH-n model to investigate the effect of boundary conditions on the profiles of zeta potential and v^z when $\zeta = 0.5$ and $\partial\phi/\partial z = 100$. Fig. 1a and b show that both the Dirichlet boundary conditions and the Neumann boundary conditions yield exactly the same ψ and v^z profiles for the NP model and the DH model at $(\alpha,\beta) = (0.05, 10^3)$ and $(1.0, 10^6)$. In the sequel, we adopt the Dirichlet boundary conditions for the NP and the DH models. Fig. 2 shows the comparison of NP, DH and PB models for various values of (α,β). Compared to the NP-d model, which is the exact model for the electroosmotic flows, Fig. 2a and b show that the PB model yields inaccurate results when the electric double layer overlaps at the center

of the channel, which occurs at small values of (α, β), while the DH model yields accurate results. On the other hand, at large values of (α, β) the DH model yields inaccurate results but the results of the PB model coincide with those of the exact NP model as depicted in Fig. 2d. These results are consistent with the basic assumptions for the PB model and the DH model specified in the Section 2, where it is reasoned that the PB model can be derived from the NP model under the conditions that $\nabla\psi = 0,\ \psi = 0,\ \nabla n^{\pm} = 0$ and $n^{\pm} = 1$ at

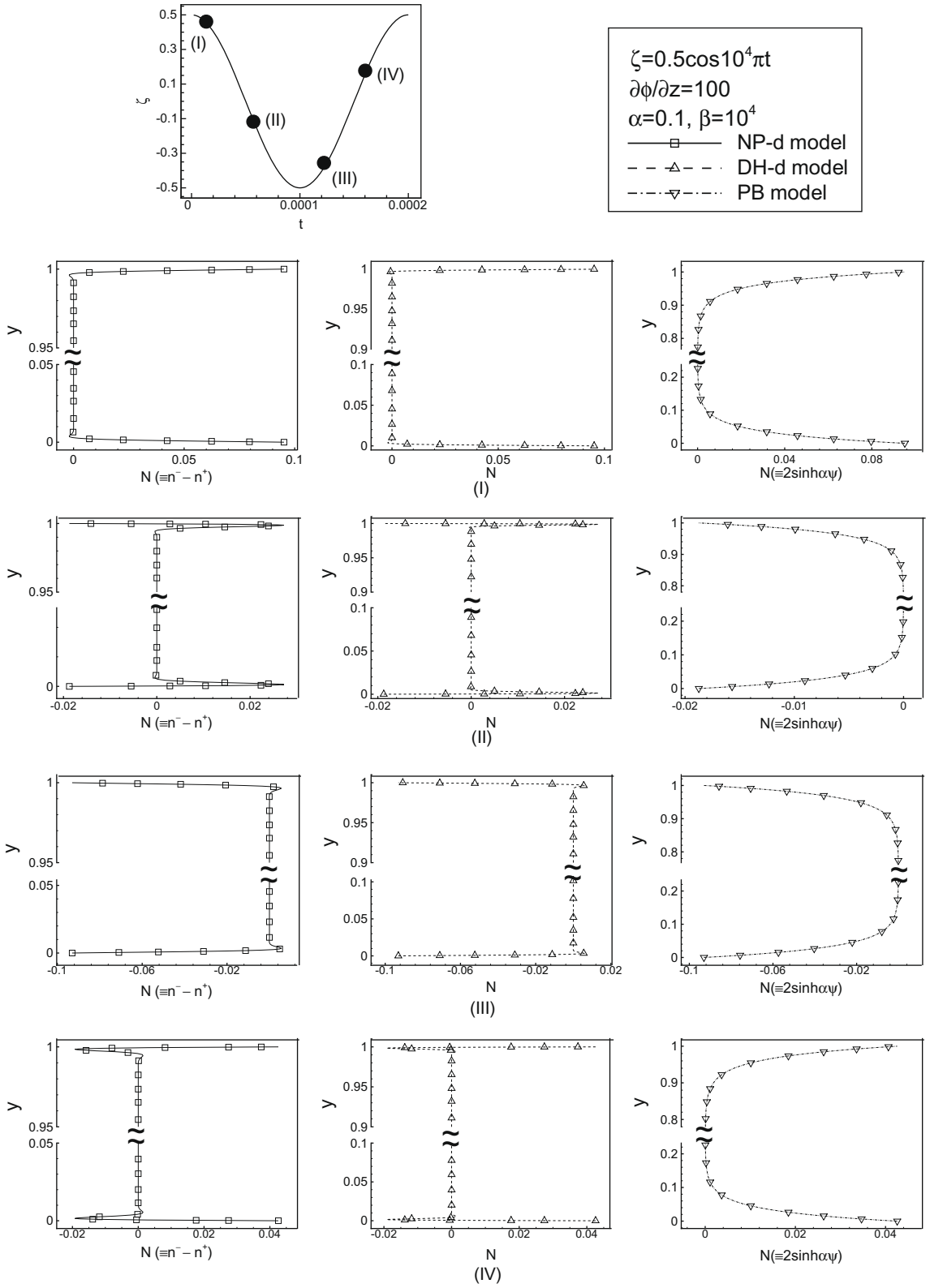

Fig. 5. Comparison of the *N*, equivalently the electroosmotic force, predicted by various models when $\zeta = 0.5\cos 10^4 \pi t$ and $(\alpha, \beta) = (0.1, 10^4)$.

the far field from the channel walls, which is tantamount to non-overlapping of EDL, and the DH model can be derived from the NP model when α is small.

Next, we consider cases where the zeta potential varies sinusoidally. Fig. 3a–c show the results of the NP-d model, the PB model and the DH-d model at the stationary state when $\zeta = 0.5\cos\omega t$ with $(\alpha,\beta) = (0.1, 10^4)$, where $\omega = 10^{-2}\pi$ (Fig. 3a), $\omega = 10\pi$ (Fig. 3b) and $\omega = 10^4\pi$ (Fig. 3c). When $\omega = 10^{-2}\pi$ the ionic distributions in the electric double layer are almost in equilibrium due to the slow variation of zeta potential, and Fig. 3a shows that the PB model and the DH-d model predict accurate results as in steady case depicted in Fig. 2c. At this slow variation of the zeta potential the dynamic behavior of ionic distributions, predicted by Eqs. (19)–(21) or Eqs. (26) and (27), does not appear and the prediction of the PB model which assumes equilibrium ionic distributions is almost the same as that of the exact NP model. Since the value of (α,β) pair

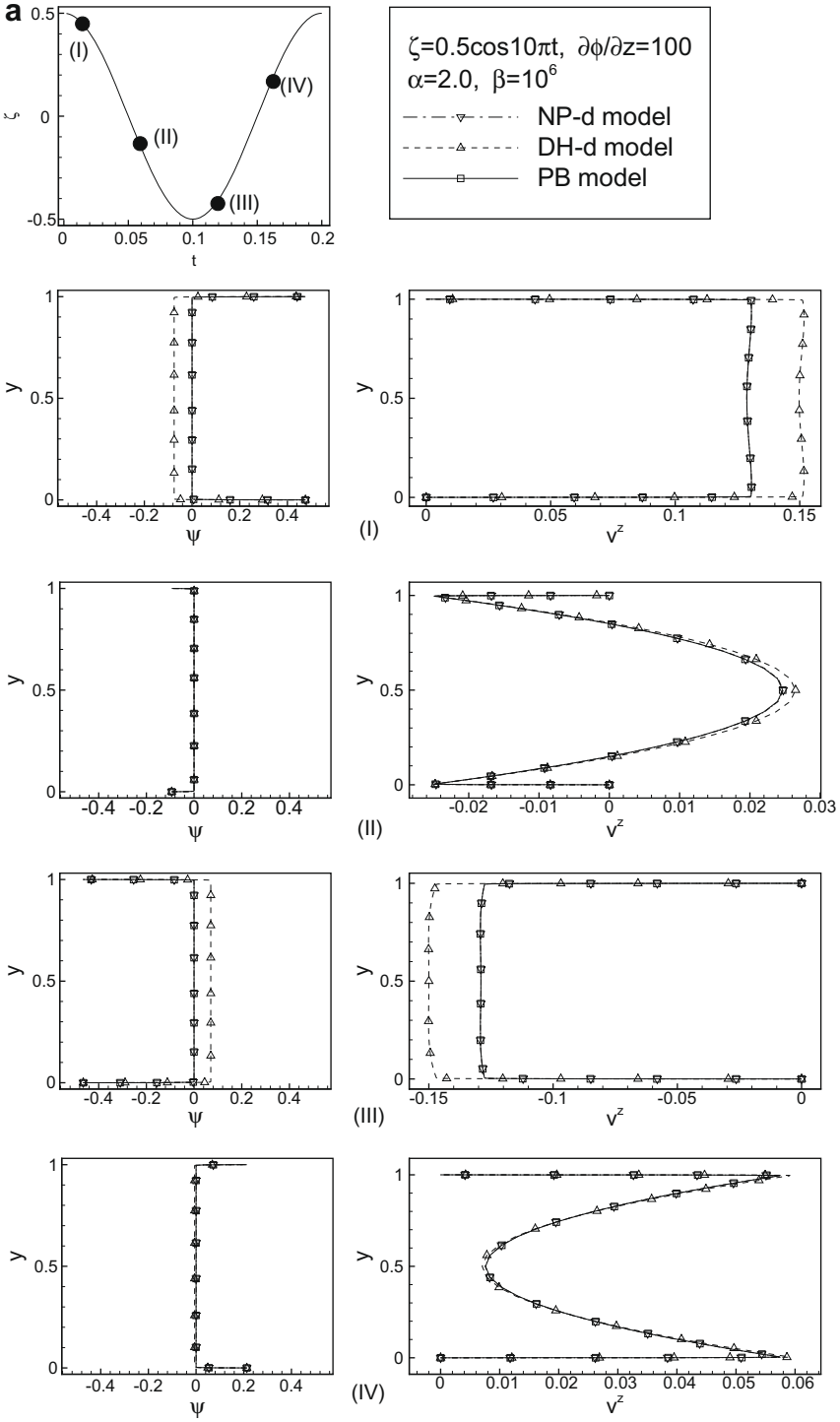

Fig. 6. (a) Comparison of the induced electric potential ψ and v^z predicted by various models when $\zeta = 0.5\cos 10\pi t$ and $(\alpha,\beta) = (2.0, 10^6)$. (b) Comparison of the induced electric potential ψ and v^z predicted by various models when $\zeta = 0.5\cos 100\pi t$ and $(\alpha,\beta) = (2.0, 10^6)$. (c) Comparison of the induced electric potential ψ and v^z predicted by various models when $\zeta = 0.5\cos 10^4\pi t$ and $(\alpha,\beta) = (2.0, 10^6)$. (d) Comparison of the induced electric potential ψ and v^z predicted by various models when $\zeta = 0.5\cos 10^6\pi t$ and $(\alpha,\beta) = (2.0, 10^6)$.

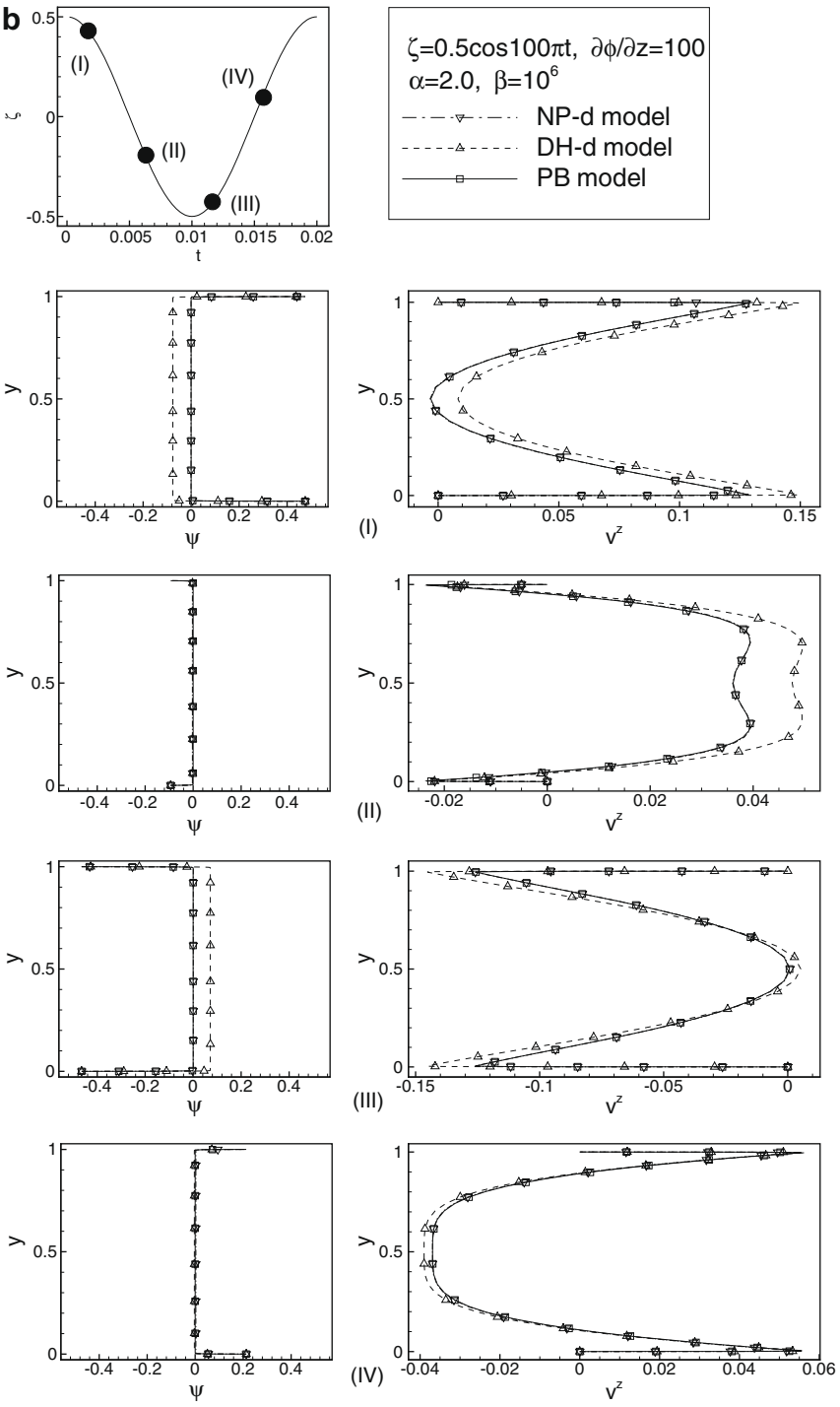

Fig. 6 (*continued*)

is small the DH model also yields accurate result. However, if ω increase to 10π the PB model based on the equilibrium ionic distribution yields quite inaccurate results when compared to those of the exact NP-d model as shown in Fig. 3b. Fig. 3b shows that the DH-d model yields accurate results at this small value of $(\alpha,\beta)=(0.1,10^4)$ since it can also take care of the dynamics of cations and anions. At a very high frequency of $\omega=10^4\pi$, the discrepancy between the NP-d model and the PB model becomes more apparent as depicted in Fig. 3c. If the dynamics of ions is taken into consideration as in the NP-d and the DH-d models, Fig. 3b and c show that the predicted induced electric potential ψ outside the electric double layer has nonzero values at $\omega=10\pi$ and $\omega=10^4\pi$, and it oscillates in accordance with the ζ variation, resulting in different v^z profiles from those predicted by the PB model. At $\omega=10^4\pi$, it should be noted that the exact ψ profile predicted from the NP-d and the DH-d models is a plug profile, which is quite different from the one predicted by the PB model. The velocity v^z predicted by the NP-d and the DH-d models is almost zero contrary to the incorrect nonzero v^z profiles of the PB model. To investigate this phenomenon further, we plot n^+, n^- and $N\equiv n^- - n^+$ obtained from the NP-d model at several instants for $\omega=10\pi$ and $\omega=10^4\pi$ in Fig. 4a and b. These figures show that

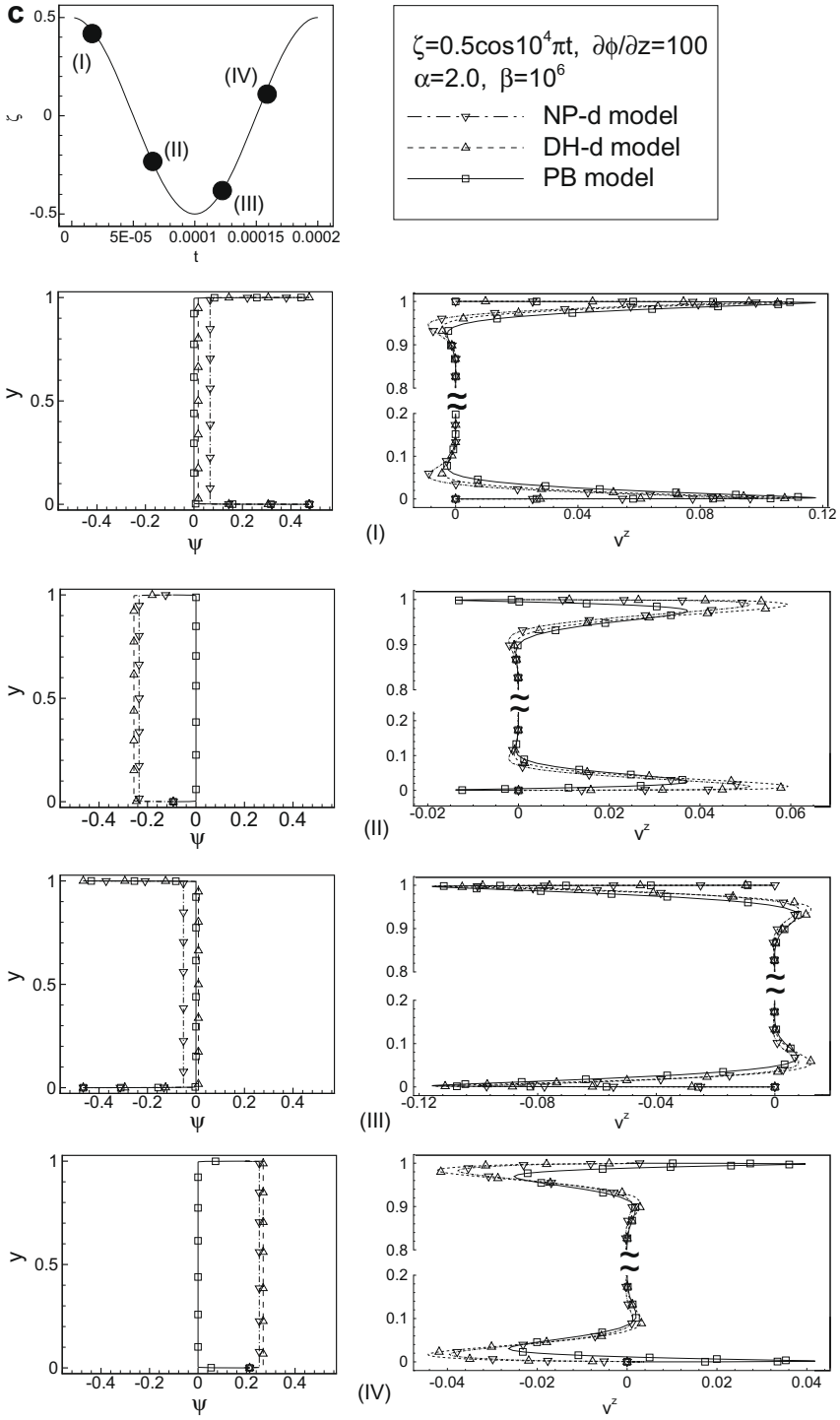

Fig. 6 (*continued*)

the concentrations of the cations and the anions deviate from unity and oscillate in accordance with the zeta potential only near the walls, resulting in vanishing value of $N(\equiv n^- - n^+)$ over the domain except within the concentration boundary layer near the walls. As the frequency ω increases from 10π to $10^4\pi$, the concentration variation at the wall cannot propagate fully into the domain, and thus the thickness of the concentration boundary layer of N is reduced. Since the driving force for electroosmotic flow is expressed as $\delta N \frac{\partial \phi}{\partial z}$ (cf. Eqs. (22) and (28)), the magnitude of v^z diminishes as ω increases. Contrary to the NP and the DH models, the PB model always assume equilibrium profiles for the ions, resulting in a large value of electroosmotic body force and consequently a large v^z value over much wider flow domain. Fig. 5 shows the N distribution, which are equivalent to the electroosmotic body force in each model, for the NP, the DH and the PB models when $\omega = 10^4\pi$. This plot apparently reveals that the PB model incorrectly predicts a larger electroosmotic body force at $\omega = 10^4\pi$, resulting in a large v^z value as shown in Fig. 3c.

Results for the case where the (α, β) value is $(2.0, 10^6)$, which corresponds to a very small Debye length, are presented in

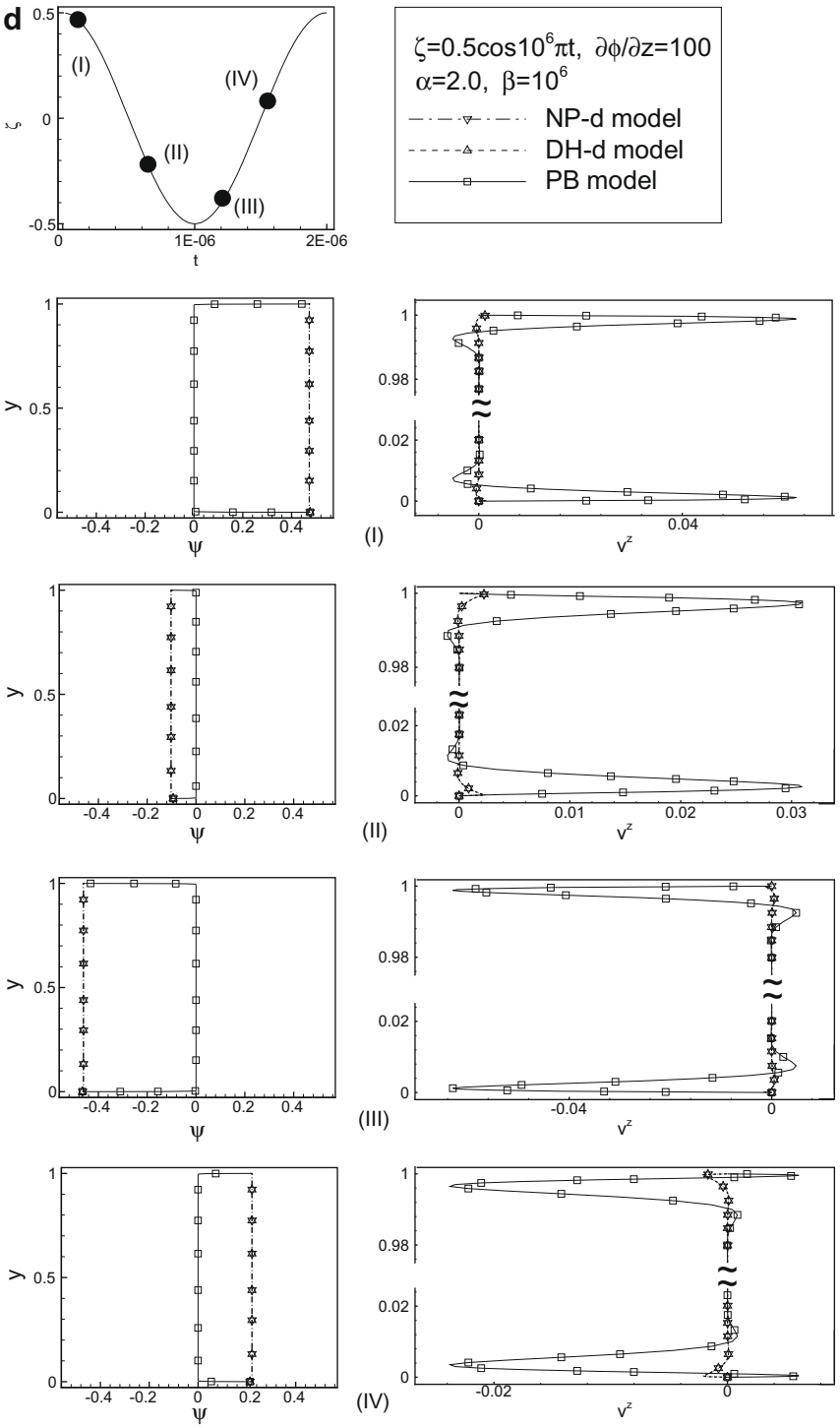

Fig. 6 (*continued*)

Fig. 6a–d. For $\alpha = 2.0$, which corresponds to a large value of zeta potential, the Debye–H"uckel model becomes inaccurate and the PB model yields results consistent with the NP model at low frequencies of $\omega = 10\pi$ and $\omega = 100\pi$ as plotted in Fig. 6a and b. As the frequency increase to $\omega = 10^4\pi$ (Fig. 6c), the dynamic behavior of ions becomes important and the PB model which assume equilibrium profiles of ions predicts quite inaccurate results. The DH model, although it can take care of the dynamic behavior of ions, yields inaccurate results because the large value of α or zeta potential invalidates the DH model. However, contrary to the case of $(\alpha, \beta) = (0.1, 10^4)$ (cf. Fig. 3c), the exact NP model as well as the DH model predict large values of v^z at $\omega = 10^4\pi$ because the fast oscillation of ions in the thin concentration boundary layer near the walls induces sufficient electroosmotic driving force at this large (α, β) value. On the other hand, if the frequency increase further to $\omega = 10^6\pi$ the thickness of the concentration boundary layer becomes sufficiently thin such that the exact NP model as well as the DH model predict diminished v^z as plotted in Fig. 6d. On the other hand, the PB model incorrectly predicts still large value of v^z for $\omega = 10^6\pi$ and $(\alpha, \beta) = (2.0, 10^6)$.

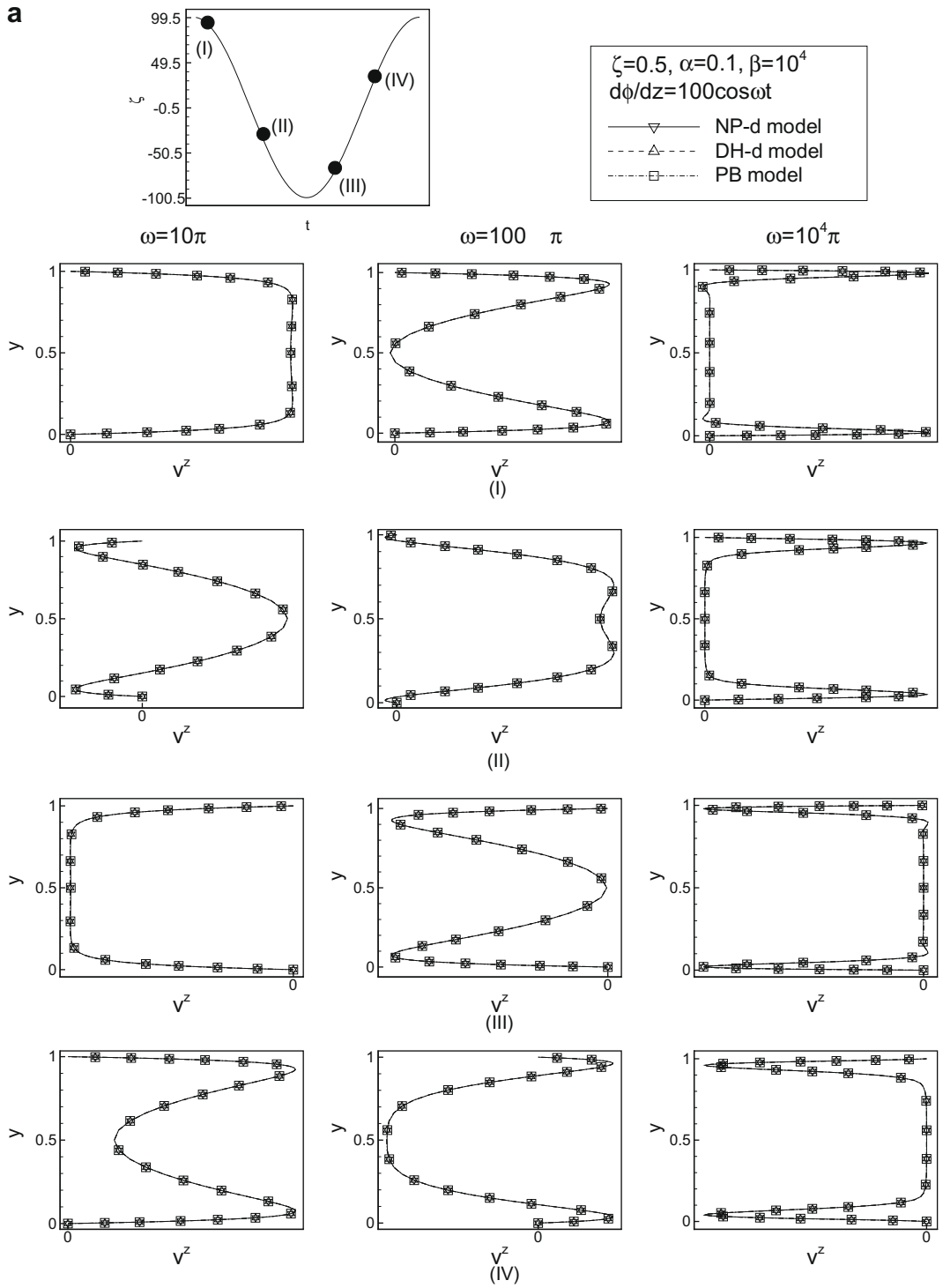

Fig. 7. (a) Comparison of various models when $\zeta = 0.5, \partial\phi/\partial z = 100\cos\omega t$ and $(\alpha, \beta) = (0.1, 10^4)$. (b) Comparison of various models when $\zeta = 0.5, \partial\phi/\partial z = 100\cos\omega t$ and $(\alpha, \beta) = (2.0, 10^6)$.

Finally, we consider the case where $\zeta = 0.5$ and $\frac{\partial\phi}{\partial z} = 100\cos\omega t$. If zeta potential is constant the external electric field $\frac{\partial\phi}{\partial z}$ cannot influence the profiles of cations and anions as expressed by Eqs. (19)–(21) and Eqs. (26) and (27). When the external electric potential is imposed along the channel walls with homogeneous zeta potential, $\frac{\partial n^{\pm}}{\partial s} = 0$ and $\frac{\partial\phi}{\partial n} = 0$ in the thin electric double layer. Here, s is the tangential direction and n is the normal direction to the wall, and $\frac{\partial\phi}{\partial s}$ is spatially constant. Then the terms $\nabla\cdot(n^{\pm}\nabla\phi)$ in Eqs. (1) and (2) become zero and the ionic distributions are not influenced by the external electric field as demonstrated in Park et al. [2]. Therefore, it is expected that the PB model yields accurate results for all values of ω when the (α, β) value is large while the DH model fails at large (α, β) value when the zeta potential is constant. Fig. 7a and b show the comparison of various models when $\omega = 10^4\pi$ and $(\alpha, \beta) = (0.1, 10^4)$ (Fig. 7a) and $(\alpha, \beta) = (2.0, 10^6)$ (Fig. 7b). At small value of (α, β), Fig. 7a shows that the v^z profiles obtained by the NP-d, the DH-d and the PB models are the same. At large value of (α, β), Fig. 7b shows that the predictions of the DH-d

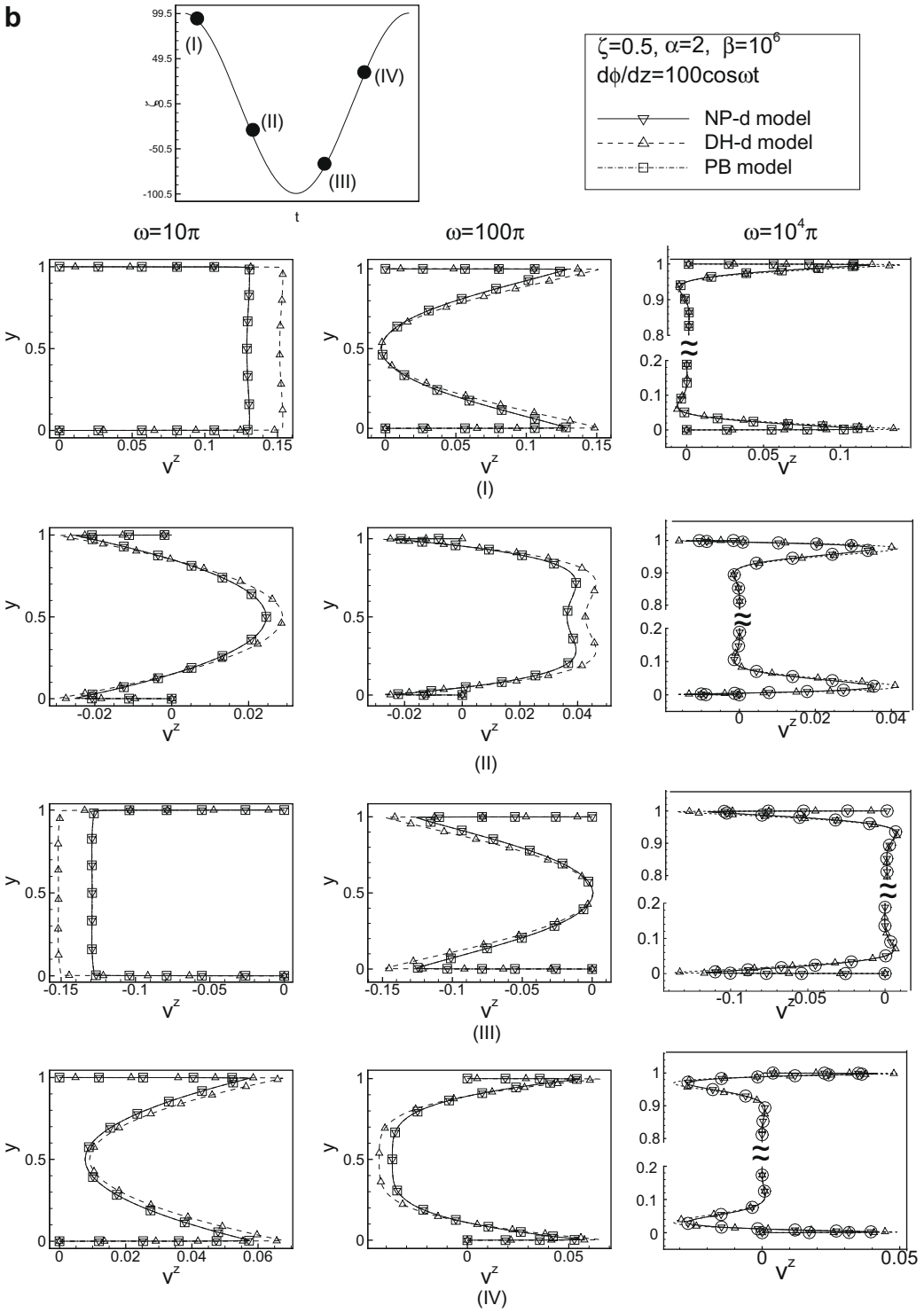

Fig. 7 (*continued*)

model are erroneous while the PB model yields results in agreement with the NP-d model for all oscillation frequencies of external electric potential.

4. Conclusion

Employing the Nernst–Planck model, the Debye–Hückel model and the Poisson–Boltzmann model, the electroosmotic flows generated by temporally varying zeta potential are investigated. The temporally varying zeta potential is recently adopted for pumping or mixing of fluids in microfluidic devices. The DH model is derived from the NP model, which is exact, under the condition of small zeta potential. On the other hand, the PB model assumes equilibrium distribution of cations and anions in the electric double layer, thus neglecting the dynamic behavior of ions. It is found that the PB model yields accurate results when the frequency of zeta potential oscillation is low, and the DH model yields accurate results for small value of zeta potential. However, for either high frequency of zeta potential oscillation or large value of zeta potential, one must adopt the NP model to get accurate predictions of electroosmotic

flows. On the other hand, for fixed value of zeta potential and oscillating external electric field, either the PB model or the DH model may be employed instead of the NP model for all oscillation frequencies of external electric field except at large values of (α, β) where the DH model breaks down.

References

[1] T. Bayraktar, S.B. Pidugu, Characterization of liquid flows in microfluidic systems, Int. J. Heat and Mass Transfer 49 (2006) 815–824.

[2] H.M. Park, J.S. Lee, T.W. Kim, Comparison of the Nernst–Planck model and the Poisson–Boltzmann model for electroosmotic flows in microchannels, J. Colloid Interface Sci. 315 (2007) 731–739.

[3] R.B.M. Schasfoort, S. Schlautmann, J. Hendrikse, A. van den Berg, Field-effect flow control for microfabricated fluidic networks, Science 286 (1999) 942–945.

[4] J.S. Buch, P.-C. Wang, D.L. DeVoe, C.S. Lee, Field-effect flow control in a polydimethylsiloxane-based microfluidic system, Electrophoresis 22 (2001) 3902–3907.

[5] C.S. Lee, W.C. Blanchard, C.T. Wu, Direct control of the electroosmosis in capillary zone electrophoresis by using an external electric field, Anal. Chem. 62 (1990) 1550–1552.

[6] M.A. Hayes, A.G. Ewing, Electroosmotic flow control and monitoring with an applied radial voltage for capillary zone electrophoresis, Anal. Chem. 64 (1992) 512–516.

[7] N.A. Mortensen, L.H. Olesen, L. Belmon, H. Bruus, Electrohydrodynamics of binary electrolytes driven by modulated surface potentials, Phys. Rev. E 71 (2005) 056306.

[8] A. Gonzalez, N.G. Green, A. Ramos, H. Morgan, A. Castellanos, Fluid flow induced by nonuniform ac electric fields in electrolytes on microelectrodes. II. A linear double layer theory, Phys. Rev. E 61 (2000) 4019–4028.

[9] N.G. Green, A. Ramos, A. Gonzalez, H. Morgan, A. Castellanos, Fluid flow induced by nonuniform ac electric fields in electrolytes on microelectrodes. III. Observation of streamlines and numerical simulation, Phys. Rev. E 66 (2002) 026305.

[10] M. Mpholo, C.G. Smith, A.B.D. Brown, Low voltage plug flow pumping using anisotropic electrode arrays, Sens. Actuators B Chem. 92 (2003) 262–268.

[11] H.M. Park, S.M. Hong, J.S. Lee, Estimation of inhomogeneous zeta potential in the electroosmotic flow by means of mode reduction, Int. J. Heat Mass Transfer 51 (2008) 176–185.